



## Full Length Article

# Prediction of flammable range of benzene/N<sub>2</sub>/O<sub>2</sub>/H<sub>2</sub>O mixtures using detailed kinetics

Alessio Frassoldati<sup>a,\*</sup>, Alaa Hamadi<sup>b</sup>, Alessandro Stagni<sup>a</sup>, Andrea Nobili<sup>a</sup>, Alberto Cuoci<sup>a</sup>, Tiziano Faravelli<sup>a</sup>, Andrea Comandini<sup>b</sup>, Nabiha Chaumeix<sup>b</sup>

<sup>a</sup> CRECK Modeling Lab, Department of Chemistry, Materials, and Chemical Engineering "G. Natta", Politecnico di Milano, P.zza Leonardo da Vinci 32, 20133 Milano, Italy

<sup>b</sup> ICARE, CNRS-INSIS, Orléans, France



## ARTICLE INFO

## Keywords:

Benzene  
Burning velocity  
Flammability limits  
Soot

## ABSTRACT

This research introduces an innovative approach to predict benzene Lower and Upper Flammability Limits (LFL and UFL). The focus of this study is on predicting the flammable range of benzene/air/steam mixtures utilizing a freely-propagating flame method, incorporating an optically-thin approximation to model soot radiation. The investigation delves into the consequences of dilution by inert gases (N<sub>2</sub> and steam), along with the impacts of pressure and initial temperature. Soot is recognized as essential not only for its role in flame chemistry under rich conditions but also for its influence on radiation, thereby affecting the flammable region of hydrocarbons especially at higher temperatures and pressures.

To address the significant formation of soot during benzene combustion near the UFL, the study integrates the kinetic model for benzene combustion with a recently developed soot mechanism based on the discrete sectional method, which has been validated extensively against a large database of sooting flames, encompassing various hydrocarbons, including benzene. To limit the computational effort associated with predicting flammability limits, a skeletal version (with 136 species and 4788 reactions) of the overall kinetic model covering benzene combustion and soot formation is developed and validated in this work.

The kinetic model was first validated against new and existing benzene flame speed data at different pressures and initial temperatures. Then it was used to investigate the flammable range. The model predictions align remarkably well with the available experimental data in the literature for the LFL, for the effect of dilution with inert gases, and with some experimental measurements for the UFL. An extensive review of these experimental data revealed significant uncertainty in characterizing benzene's UFL experimentally, both in terms of absolute value and effect of initial temperature. The comprehensive model predictions provide valuable insights, enabling differentiation among various UFL datasets for benzene.

## 1. Introduction

The utilization of a significant amount of flammable, explosive, toxic, and corrosive hazardous chemicals in industrial production processes poses significant challenges to safety management throughout various stages, including processing, production, storage, transportation, and distribution. Numerous accidents have occurred throughout the history of petrochemical and chemical process industries, prompting extensive research on evaluating and analyzing the risks associated with fires and explosions [1,2].

The flammability zone boundaries are thus very important properties

of combustible materials. Beyond the flammable boundaries, a flame cannot propagate. Thus, it is essential to keep industrial process vessels from containing fuel-oxygen-nitrogen mixtures in the flammability zone. Chemicals flammability is therefore a topic of the uttermost importance in fire safety engineering [3].

Another very important flammability property is the limiting oxygen concentration (LOC). Typically, this is the point where the upper and the lower flammability zone boundaries intersect, and it represents the lowest oxygen concentration where combustion can occur [4]. If the oxygen concentration is brought below this value, then the possibility of an explosion is removed. This reason makes the LOC essential

\* Corresponding author.

E-mail address: [alessio.frassoldati@polimi.it](mailto:alessio.frassoldati@polimi.it) (A. Frassoldati).

<https://doi.org/10.1016/j.fuel.2024.131963>

Received 5 February 2024; Received in revised form 14 May 2024; Accepted 16 May 2024

Available online 27 May 2024

0016-2361/© 2024 The Authors. Published by Elsevier Ltd. This is an open access article under the CC BY license (<http://creativecommons.org/licenses/by/4.0/>).

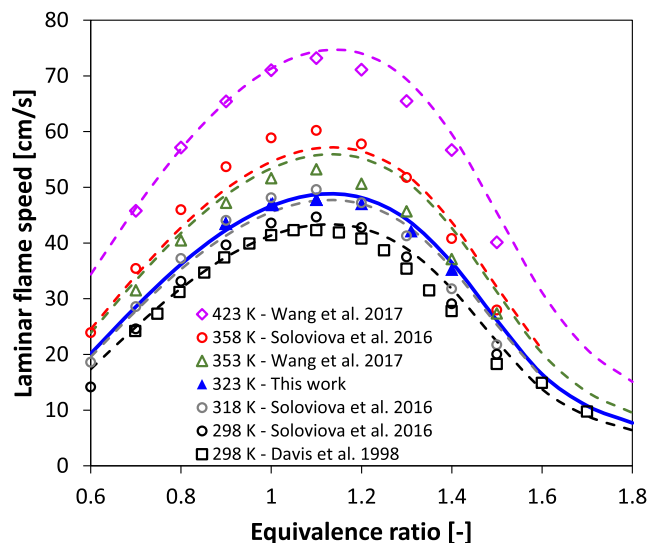


Fig. 1. Benzene/air flame speed as a function of the initial temperature:  $P = 1$  atm and  $T = 298$  K [25,26], 318 K [25], 323 K (this work), 353 K [24], 358 K [25] and 423 K [24].

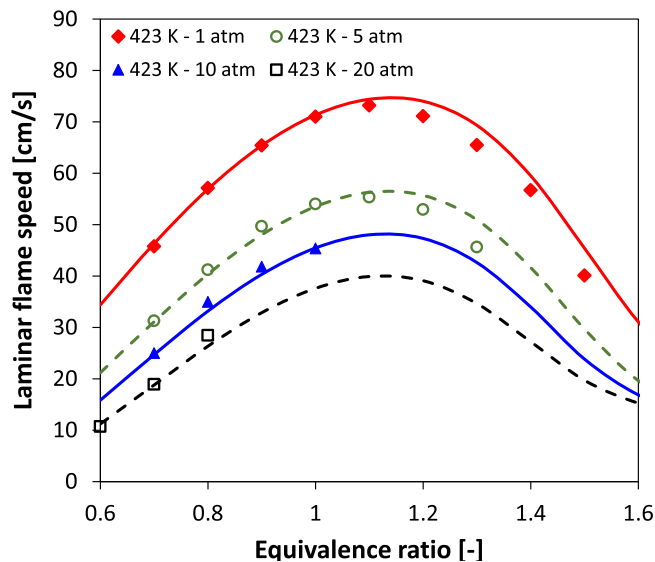


Fig. 2. Benzene/air flame speed at  $T = 423$  K and different initial pressures [24].

knowledge for inerting and purging operations.

Mendiburu et al. [5] recently provided a comprehensive review on theory, experiments, and estimation methods for flammability limits. Referring to the modelling approaches, they reviewed the literature related to the use of detailed kinetic mechanism and thermal radiation for the prediction of flammability limits. A notable finding is that nowadays, after decades of combustion research, the scientific community developed validated kinetic mechanisms for a very large number of fuels, including oxygenated fuels [6], hydrogen, ammonia [7], inert species, and their mixtures. These mechanisms include low temperature (cool flames) kinetics [8], and can also be coupled with soot formation mechanisms, thus allowing for predictive flammability limits simulations in a wide range of operating conditions and fuel composition.

Benzene is one of critical chemical raw materials and solvents widely used in various industries. Benzene poses significant risks due to their high flammability and strong toxicity. Multiple sources have published data on the flammability limits of benzene across different temperatures,

ranging from ambient to elevated levels. However, due to variations in measurement methods and accuracy, the mentioned literature exhibits important experimental data discrepancies, particularly concerning the UFLs. Since adding diluents is one of common methods to prevent explosions and extinguish fires, different authors also investigated the effect of common diluents such as  $N_2$ , and steam ( $H_2O$ ) [2,9]. Preventing these accidents is necessarily associated to the capability of anticipating the occurrence of such events, which implies their understanding at a fundamental level. This is done in this paper via chemical kinetics and flame simulations.

In summary, the present work first develops and extensively validates a skeletal kinetic mechanism able to describe benzene combustion even in rich and ultra-rich conditions, i.e. where a significant formation of soot is present. The model is validated using a large set of literature experimental data of benzene combustion, including JSR and premixed flames, as well as flame speed measurements. The collection of benzene flame speed measurements available in the literature is complemented by a new set of measurements obtained at CNRS and presented in this paper. The comparison with flame speed measurements is discussed in this paper, while the complete validation with other literature data is presented in the [Supplementary Material](#).

## 2. Methodology

### 2.1. Flame speed measurement of benzene/air flames at 1 atm and 323 K

Unstretched laminar flame speeds  $s_L^0$  have been measured in the ICARE-CNRS BS-II spherical bomb described in [10]. The large size of the facility allows the measurements of expanding spherical flames, spark ignited at the center, up to a diameter of 97 mm with no increase of the initial pressure. This is verified for each run via the monitoring of the pressure inside the vessel via a piezo-electric pressure transducer (Kistler 601A). The expanding flame is recorded via a high-speed camera (Phantom v1611) with a framing rate of 19,004 and 25,000 fps. A homemade imaging processing system is used to extract the flame radius and hence obtain the flame trajectory  $r_{flame} = f(\text{time})$ .  $s_L^0$  is extracted from the flame radius using the non-linear expression of the flame speed versus stretch rate. More details are available in [11,12]. The initial temperature was fixed at  $50 \pm 0.5$  °C thanks to the regulation of a thermo-fluid heating system. The benzene is manufactured by Sigma-Aldrich ( $\geq 99.9\%$ ). The synthetic air is composed of 20.9 %  $O_2 + 79.1\%$   $N_2$  (Air Liquide, grade alphagaz 2, purity  $> 99.9999\%$ ). The combustible mixture is directly made inside the facility using the partial pressure method. The partial pressure and total pressure are read via capacitive gages, MKS-631, with suitable ranges (100 Torrs and 1000 Torrs full scales). According to the precision of the manometers, the mixtures were obtained with an accuracy of 99.5 %.

### 2.2. Kinetic mechanism development

The kinetic mechanism developed at the CRECK Modeling Lab at Politecnico di Milano is used to describe the chemistry of benzene combustion. The mechanism is freely available in CHEMKIN format at the following web address: <https://creckmodeling.chem.polimi.it/>. The accuracy of this mechanism in predicting speciation data and flame speed for a large number of fuels and fuel mixtures and different operating conditions has been previously demonstrated [13,14]. The kinetic model for soot formation, which was added to the kinetic mechanisms used in this study, is the latest version of the soot sectional model of Nobili et al. [15], which has been extended to include soot aggregates with sizes up to 9  $\mu m$ .

The kinetic scheme was reduced starting from a comprehensive kinetic model, including 327 species and 13,417 reactions by adopting the DoctorSMOKE++ code [16]. The obtained skeletal mechanism is available as [supplementary Material](#) and contains 136 species (53 of them are

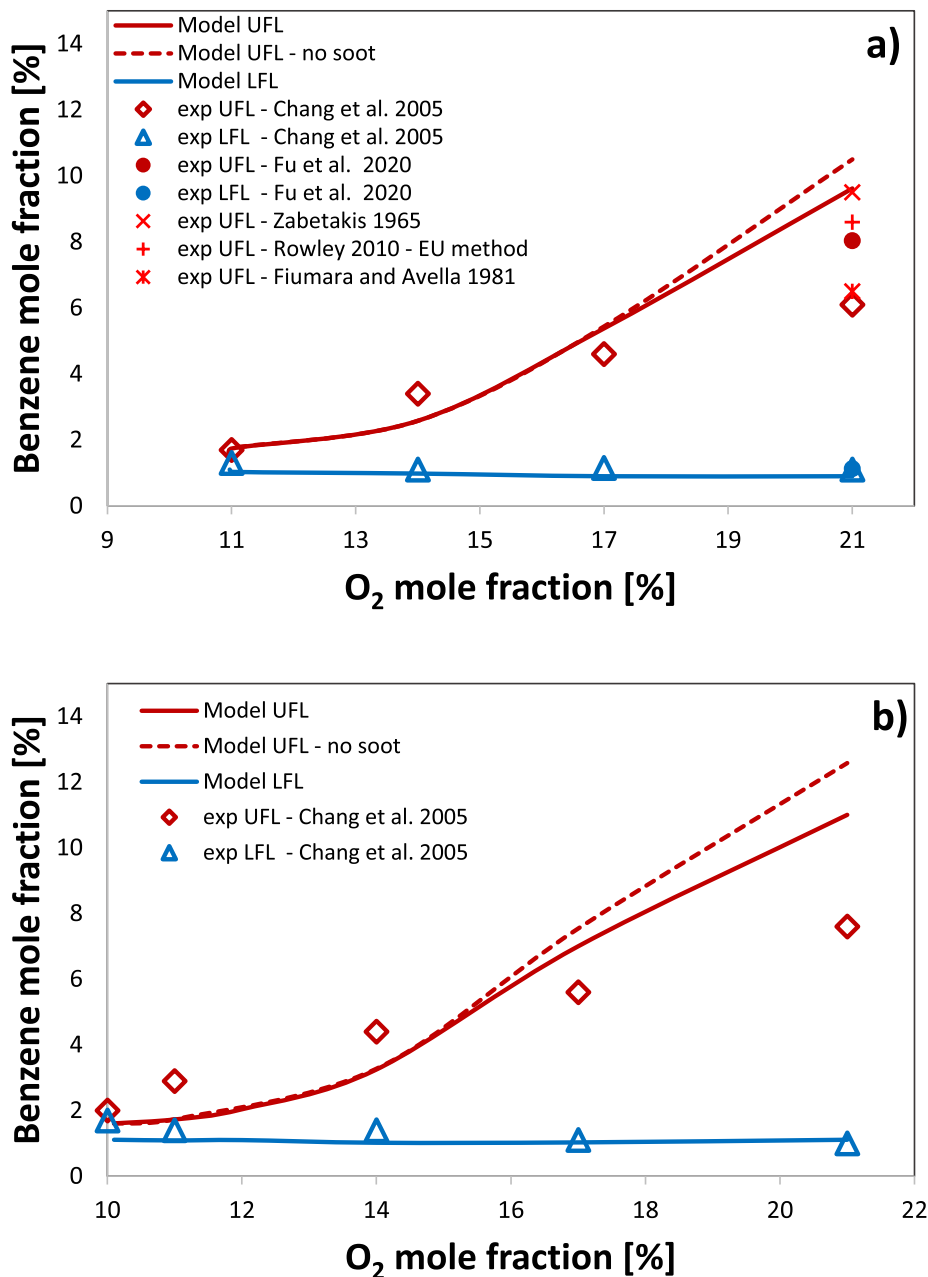


**Fig. 3.** Benzene/O<sub>2</sub>/N<sub>2</sub> flammable range at 423 K and 1 (Panel a) and 2 atm (Panel b). Comparison between model predictions and experimental measurements [1,2,9,27,28].

BINs, i.e. species representing large PAHs and soot particles) involved in 4788 reactions. While the focus of this paper is on benzene flammability, the overall methodology and the soot mechanism are general and can be utilized also with different fuels as discussed by Bertolino et al. [3] and Nobili et al. [15].

### 2.3. Flame speed and flammability limits simulations

All the simulations reported in this study were carried out using the OpenSMOKE++ Suite framework [17] and adopting the skeletal mechanism presented in the previous paragraph. The OpenSMOKE++ Suite was adopted first to validate the kinetic mechanism and then to calculate the flammability limits (LFL, UFL) using a 1D system corresponding to a non-adiabatic freely-propagating flame (FPF), as described in detail in [3]. A 10 cm computational domain was adopted,

with a large number of grid-points (up to 1,000) to ensure accurate and grid-insensitive results. In a similar work for methane, Mascarenhas et al. [18] used 400 grid points. In this study, a radiative term ( $\dot{Q}_{rad}$ ) is considered in the energy conservation equation to account for the flame heat losses. The importance of radiation heat losses at low flame speeds, i.e. below  $\sim 10$  cm/s, has been recognized and discussed by several authors [19,20,21]. The model incorporates the optically thin approximation, which is mathematically expressed by the Equation (1):

$$\dot{Q}_{rad} = 4\sigma \left[ \sum_{k=1}^{N_s} p_k \alpha_k + \delta \right] (T^4 - T_{env}^4) \quad (1)$$

where  $\sigma$  is the Stefan–Boltzmann constant,  $p_k$  and  $\alpha_k$  the partial pressure and the Planck mean absorption coefficient for the  $k^{\text{th}}$  species, respectively, and  $\delta$  is soot emissivity. The radiative properties of gases are

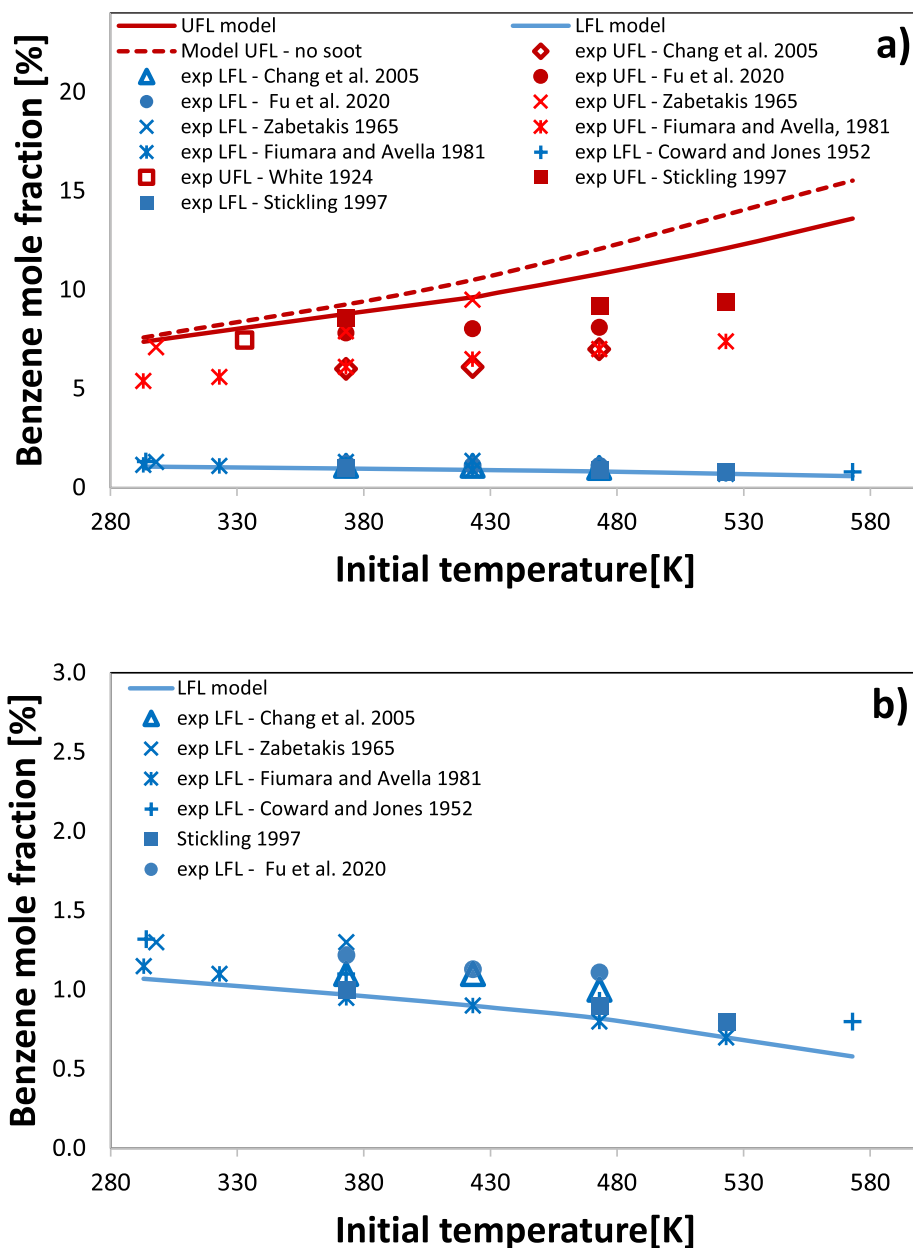


Fig. 4. Benzene/air flammable range at 1 atm and different initial temperature. Comparison between model predictions and experimental measurements [1,2,9,27,31,32,33]. Panel b) shows the detail of the LFL limit.

based on the RADCAL model [22]. Since the predictions of the UFL require the simulation of a rich flame, a soot emissivity model is included in the present work, through Equation (2):

$$\delta = C f_v T \quad (2)$$

where  $T$  is the temperature,  $f_v$  is the soot volumetric fraction, and  $C$  is a fitting constant whose value ( $C = 2370 \text{ 1/m/K}$ ), estimated by Widmann [23]. The flammability limits are calculated without using any “threshold flame temperature” or “limiting burning velocity”. The mixture composition at the point of the last burning flame before flame extinction determines both flammability limits [3].

### 3. Results and discussion

#### 3.1. Flame speed

Fig. 1 shows a comparison between model predictions and flame speed measurements for benzene/air flames measured by different authors at different initial temperatures. The agreement between model predictions and experimental results is satisfactory in the entire range of conditions investigated. In general, literature data present a certain degree of uncertainty.

The model tends to overestimate the data of Wang et al. [24], and underestimate those of Soloviova–Sokolova et al. [25], while it agrees with the data of Davis et al. [26] and the new measurements of CNRS (this work) at 323 K.

Fig. 2 shows that the model is capable of predicting the effect of pressure on benzene flame speed in air.

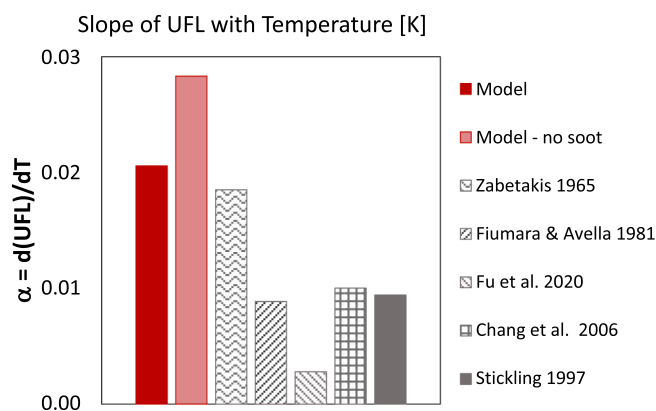


Fig. 5. Slope of the linear trend of UFL with temperature. Comparison between model predictions and experimental measurements [1,2,9,27,31].

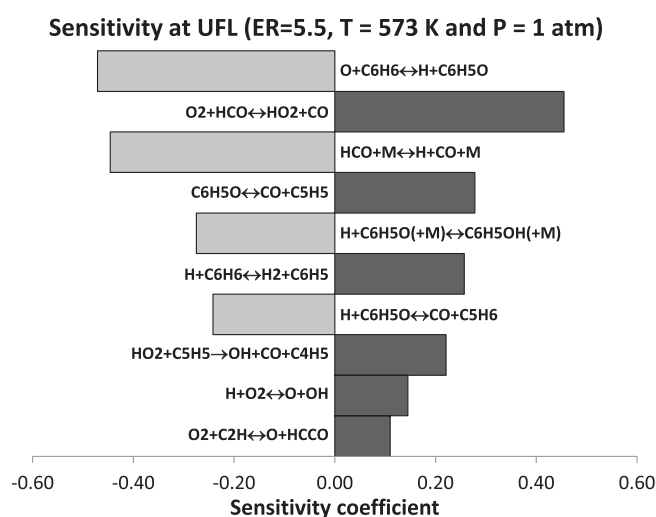


Fig. 6. Benzene/Air flame speed at P = 1 atm and T = 573 K. Sensitivity analysis close to UFL.

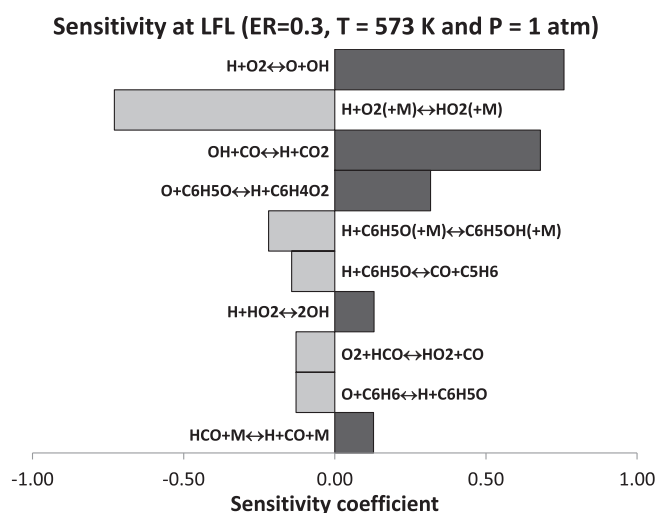


Fig. 7. Benzene/Air flame speed at P = 1 atm and T = 573 K. Sensitivity analysis close to LFL.

### 3.2. Prediction of benzene flammability limits

The FPF model employs a kinetic mechanism to describe the structure of a laminar flame, which is steady, non-adiabatic, 1D and planar, resulting in an accurate description of the phenomena involved in flame propagation and extinction [3].

Starting from stoichiometric conditions, the FPF flame model dynamically solves the evolving flame structure when the equivalence ratio ( $\phi$ ) is slowly increased (or decreased) until flame extinction is observed. We adopted the suggestion of Smooke et al. [29], who recommended using for solving a freely propagating flame a value of the fixed temperature of 100 K above the unburned gas temperature. This ensures that also very weak freely propagating flames can be simulated until their extinction is observed. The computational mesh is also dynamically adjusted to follow the modification of the flame structure with the change of  $\phi$ . In this way, the UFL and LFL limits are evaluated. Regarding the experimental data, when different values for the flammability limits were reported for upward or downward propagation, the value for the upward propagation has been selected. In fact, the UFLs determined with downward flame propagation (DFP) are smaller due to buoyancy effects [5]. Fig. 3 illustrates how the flammability limits of benzene at 423 K and 1 or 2 atm are affected by the composition of the oxidizer (O<sub>2</sub>/N<sub>2</sub> mixture).

Various authors have reported different measured values for the air (21 % O<sub>2</sub>) case, underscoring the inherent uncertainty of this type of experimental measurements for the UFL. In these conditions the FPF model is more in line with the UFL measured by the US Bureau of Mines [2]. The model effectiveness in predicting the (anticipated) negligible effect of oxidizer composition on the LFL and substantial impact on the UFL is apparent. In these conditions, the model predicts a LOC of 10.95 %, in line with the experimental results of Lewis and Von Elbe (O<sub>2</sub> = 11.2 % at 1 atm and room temperature) [30].

Fig. 3 also shows that the formation of soot is negligible for diluted conditions, since extinction occurs at very slightly rich conditions where soot is not formed (in the atmospheric case at the UFL,  $\phi = 3.9$  in air and becomes  $\phi = 1.21$  in 11 % O<sub>2</sub>). The effect of soot tends to become more relevant at higher pressure. Fig. 4 illustrates how the initial temperature influences the flammable range of benzene/air mixtures. Consistent with expectations, the model anticipates a widening of the flammable range due to the elevated initial temperature. This impact is noticeable on the upper flammable limit (UFL) side of the flammable region. Panel b) of the same figure highlights the comparison between model prediction and different experimental values for the LFL. In this case the model well agrees with the experimental results of Fiumara and Avella [27] and Stickling [31].

It is crucial to note that the model aligns closely with all the experimental data available in the literature concerning the lower limit (LFL). Remarkably, there is a high level of consistency across various experimental results. In contrast, there is a notable lack of agreement among different literature results at the upper limit (UFL).

Mendiburu et al. [5] and Qi et al. [34] conducted a comprehensive review of the experimental methodologies utilized in assessing flammability limits and their associated uncertainties. Their review highlighted the dependence of flammability limits on the volume of the tube or vessel used for measurement, up to a critical volume threshold. Additionally, they observed that the direction of flame propagation (whether upward or downward) is influenced by buoyancy, particularly noticeable in the context of upper flammability limits (UFLs). It is noteworthy that the model aligns with recent data from Fu et al. [9] (at low temperatures), as well as the historical upper flammability limits (UFLs) measured by the US Bureau of Mines [2], and by White [33]. However, the data obtained by Chang et al. [1] and Fiumara and Avella [27] exhibit a notable deviation from the model, amounting to  $\sim 2.5$  % (benzene % mole fraction at the UFL).

Fig. 5 demonstrates that also the temperature trend – reflected in the slope of the linear trend obtained from the data presented in the

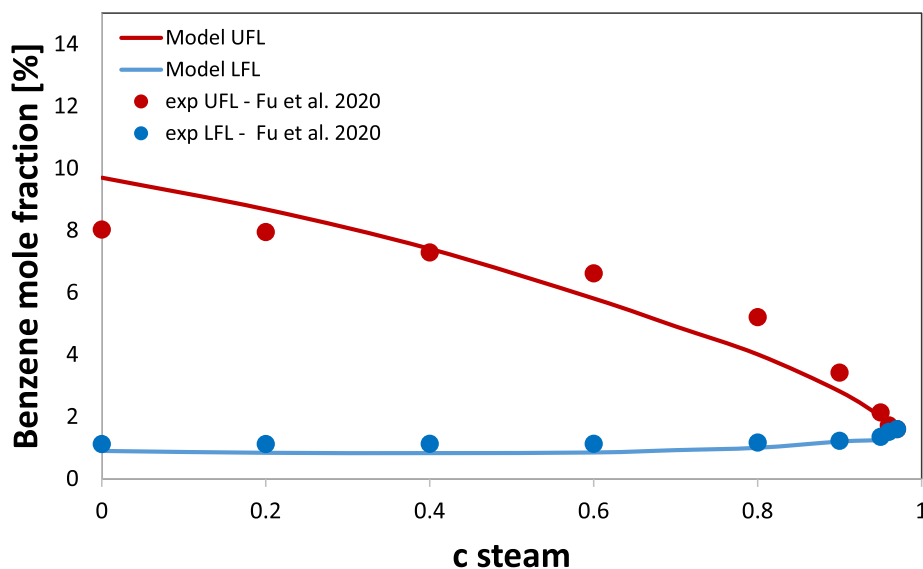


Fig. 8. Benzene/Air/H<sub>2</sub>O flammable range. Comparison between predictions and experimental data [9]. P = 1 atm, T = 423 K.

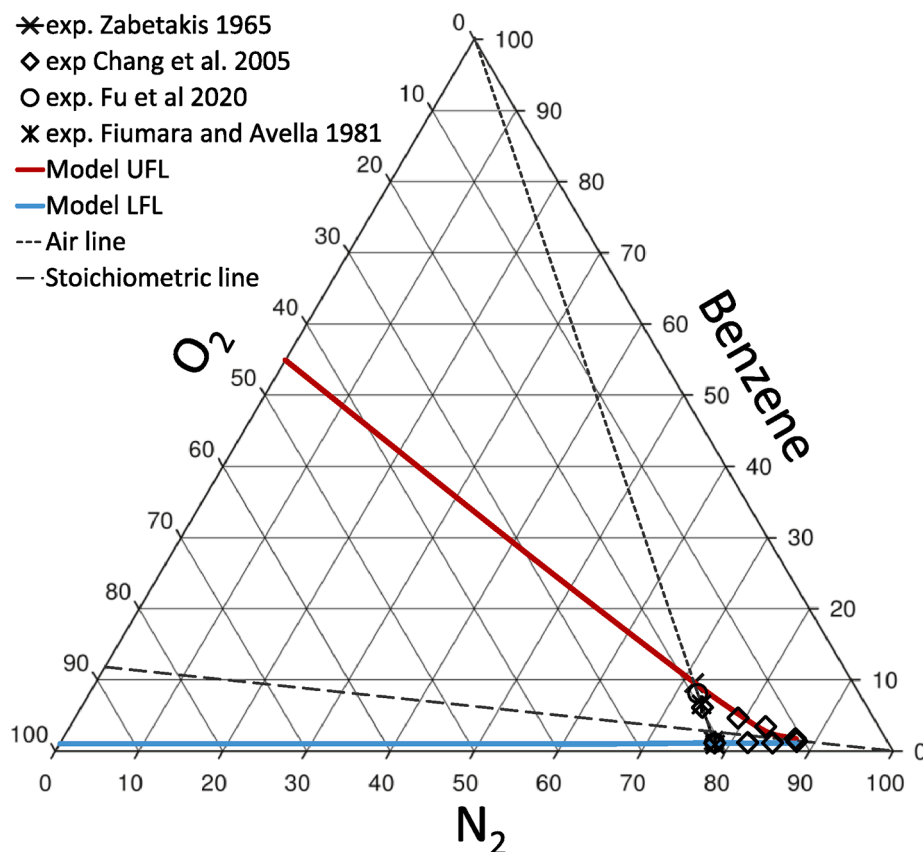


Fig. 9. Benzene/N<sub>2</sub>/O<sub>2</sub> flammable range at P = 1 atm and T = 423 K. Comparison between model predictions and experimental measurements [1,2,9,27].

experiments of Fig. 4 – as measured by these authors, does not always align with the predictions of the model. The slope  $\alpha$  is determined through a linear regression applied to either model predictions or experimental findings across the temperature range depicted in Fig. 4 (e.g. up to 523 K for both model and experiments). The inconsistency between the slope proposed by the different authors is apparent, underscoring the substantial uncertainties in these measurements, particularly

at the upper flammability limit (UFL). The model well agrees with the temperature dependence measured by Zabetakis [2] while the other authors, especially Fu et al. [9], measured a significantly lower effect of initial temperature on benzene UFL. It is imperative to thoroughly evaluate these uncertainties, given that these values are employed in extrapolating measured UFLs at higher temperatures [5]. Notably, neglecting the formation of soot leads to a significant overestimation of



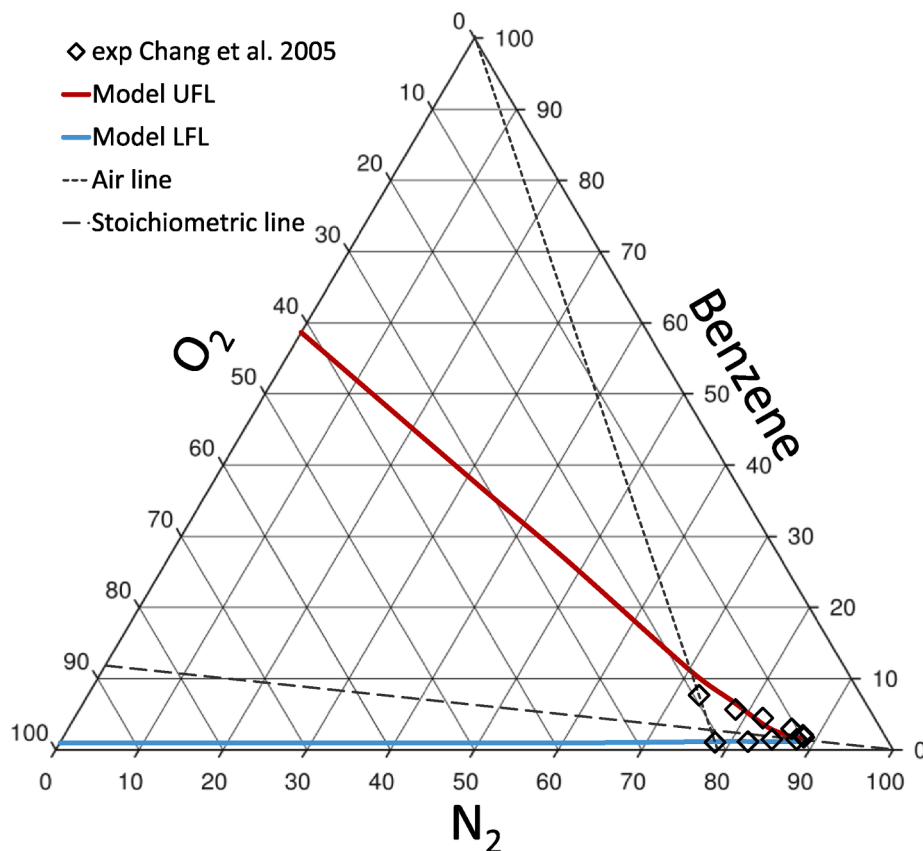


Fig. 10. Benzene/ $N_2/O_2$  flammable range. Comparison between predictions and experimental measurements [1].  $P=2$  atm,  $T=423$  K.

the effect of temperature on the UFL.

### 3.3. Kinetic and sensitivity analysis

The flame extinction conditions associated to flammable limits were clearly determined for all the conditions explored in this study. It is worthwhile to conduct a kinetic and sensitivity analysis, as these conditions differ significantly from the typical scenarios where flame speeds are calculated. The sensitivity of flame speed to specific reactions is mostly associated to the competition between branching and terminating reactions, affecting the overall radical pool and thus flame reactivity. This point was clearly addressed by Law and Egolfopoulos [35] specifically for flames in conditions close to the flammability limits. The flame temperature is naturally reduced when the flammability limit is approached. This significantly weakens the temperature-sensitive branching reactions but has a much smaller influence on the termination reactions, which generally have no activation energy. Therefore, close to the flammable limit termination reactions overwhelm branching reactions, causing a rapid slowdown of the overall reactivity and of the heat release rate, which makes the effect of heat loss even greater, finally resulting in flame extinction.

For example, Fig. 6 and Fig. 7 show the sensitivity analysis for flames very close to the extinction conditions. For the UFL, this corresponds to a very rich mixture ( $\phi = 5.5$ ), while for LFL to a very lean one ( $\phi = 0.3$ ). For both flames the maximum temperature is  $\sim 1300$  K.

It is possible to observe that the relative importance of the reactions controlling flame propagation in very rich conditions differs from that in stoichiometric benzene/air flames [13]. While the stoichiometric flame is dominated by the chain-branching  $H + O_2 = O + OH$ , followed by HCO decomposition ( $HCO + M = H + CO + M$ ) and CO oxidation ( $CO + OH = CO_2 + H$ ), in rich conditions the reactivity is controlled by the competition between two reactions involving formyl radical ( $HCO + M$

$= H + CO + M$ , and its reaction with  $O_2 + HCO = HO_2 + CO$ ). The role of phenoxy radical, already discussed in [13] at  $\phi = 1$ , remains important especially for its role in termination reactions with H radicals.

Fig. 7 shows that under extremely lean conditions, the significance of CO oxidation and the inhibitory impact of  $HO_2$  formation become apparent. It is also worth noting that at the LFL the HCO decomposition reaction promotes the reactivity and its reaction with  $O_2$  has an inhibiting effect, differently from UFL conditions. The role of the competition between formyl radical decomposition (forming the reactive H radical, leading to chain branching via  $H + O_2 = OH + O$ ) and oxidation (forming the relatively unreactive  $HO_2$  radical) has been discussed in detail by Santer et al. [36].

### 3.4. Effect of dilution and pressure

Fig. 8 shows the impact of steam dilution on the flammability limits of atmospheric benzene/air mixtures. As the quantity of steam increases, the UFL decreases, with minimal sensitivity observed in the lower limit. Beyond a certain threshold of steam content, the UFL experiences a significant reduction, while the LFL shows a slight increase. The critical flammability point is reached when the LFL equals the UFL, specifically when the steam content in the diluted fuel mixture reaches approximately 0.97 (v/v). Fig. 8 illustrates that the agreement between model predictions and experimentally measured flammability limits is satisfactory. However, the model slightly underestimates the upper flammability limit (UFL) at high steam dilutions.

In Fig. 9, a triangular diagram is utilized to present a comparison between all available experimental data at 423 K and 1 atm and the model predictions. This diagram enables the representation of model predictions up to pure oxygen. It is apparent that under these conditions, the limiting oxygen concentration (LOC) is approximately 11 %, aligning with the findings reported by Chang et al. [1].

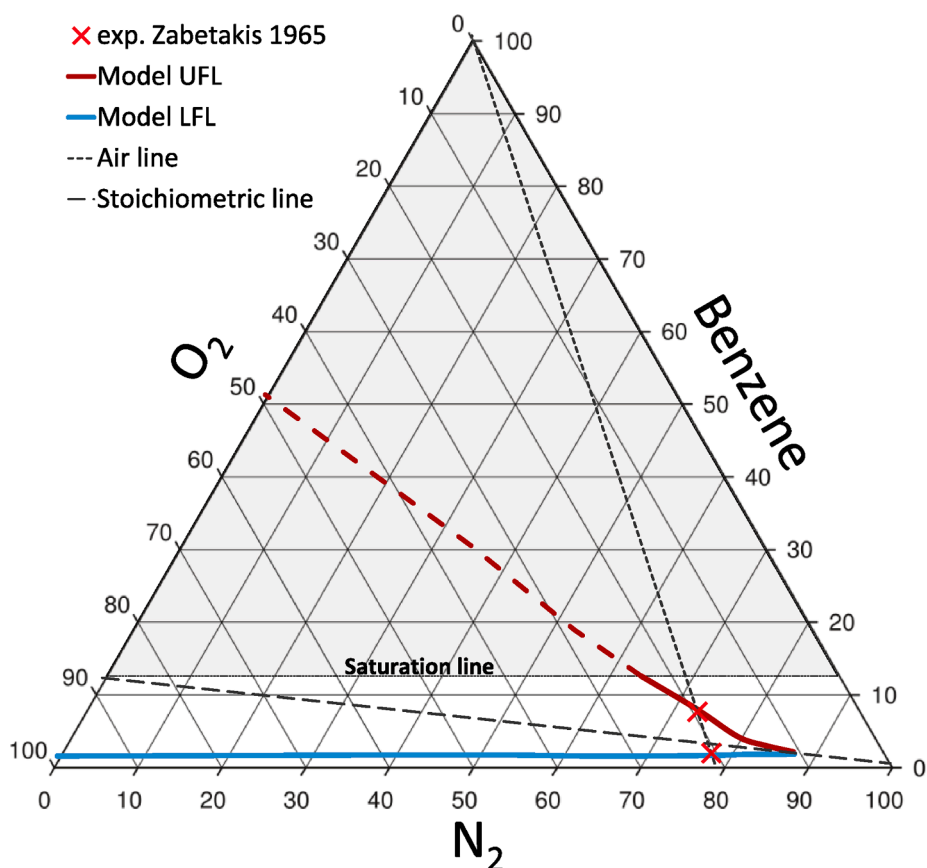


Fig. 11. Benzene/ $N_2/O_2$  flammable range. Comparison between predictions and experimental measurements [2].  $P = 1$  atm,  $T = 298$  K.

Fig. 10 shows the impact of pressure (2 atm) on the flammability region. The model successfully predicts the observed, albeit modest, increase in flammability limits, particularly for the upper flammability limit (UFL). In an air environment with 21 %  $O_2$ , the experimentally determined flammable region ranges from 1.1 % to 6.1 % (benzene mole fraction) at 1 atm and from 1.0 % to 7.60 % at 2 atm. Consequently, the measured increase in UFL due to pressure change is  $\Delta = 1.5$  %, aligning well with the model prediction ( $\Delta = 1.25$  %).

To complete the analysis, the triangular diagram at ambient conditions is provided in Fig. 11. At ambient conditions, above  $\sim 12.5$  % of benzene the system is above the saturation zone. Thus, in this zone the model results are not of significance since mists are present.

#### 4. Conclusions

This study involved the development and thorough validation of a skeletal kinetic mechanism, utilizing both literature experimental data and new measurements of benzene/air flame speed at 323 K and atmospheric conditions. The model incorporates a soot sub-section to enable the modeling of rich and ultra-rich conditions. While initially tailored for benzene, the model's adaptability allows for easy extension to encompass various fuels and fuel mixtures, leveraging the extensive investigation of numerous fuel species by the CRECK Modeling Lab.

The Freely Propagating Flame (FPF) approach was employed to predict the flammability limits of benzene/air mixtures. This approach considers the impact of inert dilution and includes the influence of soot on radiation and subsequent flame extinction. Flame propagation is significantly influenced by radiation, particularly in limit mixtures characterized by low reactivity. Previous research highlights the importance of incorporating a soot sub-mechanism and radiation model, particularly for the Upper Flammability Limit (UFL), a factor prominently relevant to benzene flames even under atmospheric pressures.

This significance becomes more pronounced at higher pressures.

The model effectively predicted the flammable range not only for benzene/air mixtures but also for mixtures diluted with  $N_2$  and  $H_2O$ , as well as the effects of pressure. Notably, available UFL data are marked by considerable uncertainty. In this context, the model serves as a valuable tool to discern among these data points and identify systematic deviations.

Finally, the model was applied to assess the flammability triangle diagram for benzene/ $N_2/O_2$  under varying initial temperatures and pressures. The model has been validated and thus can be utilized to evaluate the flammability regions of Benzene/ $O_2/N_2$ /dilutants in different conditions, e.g. higher pressures and initial temperatures where the importance of the soot sub mechanism is anticipated to be even larger. The same methodology can be applied to different fuels and their mixtures, also in the case of non-conventional oxidizers (e.g.,  $N_2O$ ), as well as for different diluents and/or flame retardants (e.g., fluorinated compounds), for which a validated kinetic mechanism is available.

#### CRediT authorship contribution statement

**Alessio Frassoldati:** Writing – original draft, Supervision, Methodology, Investigation, Conceptualization. **Alaa Hamadi:** Investigation, Data curation. **Alessandro Stagni:** Methodology, Formal analysis. **Andrea Nobili:** Investigation, Data curation, Conceptualization. **Alberto Cuoci:** Writing – review & editing, Software, Conceptualization. **Tiziano Faravelli:** Writing – review & editing, Supervision, Conceptualization. **Andrea Comandini:** Investigation, Data curation, Conceptualization. **Nabiha Chaumeix:** Investigation, Data curation, Conceptualization.



## Declaration of competing interest

The authors declare that they have no known competing financial interests or personal relationships that could have appeared to influence the work reported in this paper.

## Data availability

All data are shared as [Supplementary Material](#) files

## Appendix A. Supplementary data

SM-1: skeletal kinetic mechanism for benzene combustion including soot formation; SM-2: extensive validation of the complete and skeletal kinetic mechanisms using literature data (JSR, premixed 1D flame etc.). SM-3: supplemental material on flame speed measurements. Supplementary data to this article can be found online at <https://doi.org/10.1016/j.fuel.2024.131963>.

## References

- Chang YM, Tseng JM, Shu CM, Hu KH. Flammability studies of benzene and methanol with various vapour mixing ratios at 150 °C. *Korean J Chem Eng* 2005; 803–12.
- Zabetakis MG. *Fire and Explosion Hazards at Temperature and Pressure Extremes*. AIChE-ICHEME Symp Ser 1965;2:99–104.
- Bertolino A, Stagni A, Cuoci A, Faravelli T, Parente A, Frassoldati A. Prediction of flammable range for pure fuels and mixtures using detailed kinetics. *Combust Flame* 2019;207:120–33.
- Crowl DA, Louvar JA. *Chemical Process Safety: Fundamentals with Applications*. Upper Saddle River, NJ: Prentice Hall Inc; 2001.
- Mendiburu AZ, Jr JAC, Ju Y. Flammability limits: a comprehensive review of theory, experiments, and estimation methods. *Energy Fuels* 2023;37(6):4151–97.
- Ranzi E, Frassoldati A, Stagni A, Pelucchi M, Cuoci A, Faravelli T. Reduced kinetic schemes of complex reaction systems: fossil and biomass-derived transportation fuels. *Int J Chem Kinet Sep*. 2014;46(9):512–42. <https://doi.org/10.1002/kin.20867>.
- Stagni A, Arunthanayothin S, Dehue M, Herbinet O, Battin-Leclerc F, Bréquigny P, et al. Low- and intermediate-temperature ammonia/hydrogen oxidation in a flow reactor: experiments and a wide-range kinetic modeling. *Chem Eng J Sep*. 2023; 471:144577. <https://doi.org/10.1016/j.cej.2023.144577>.
- Liang W, Law CK. Extended flammability limits of n-heptane/air mixtures with cool flames. *Combust Flame Nov*. 2017;185:75–81. <https://doi.org/10.1016/j.combustflame.2017.06.015>.
- Fu W, Zhang K, Wu J. Flammability limits of benzene, toluene, xylenes from 373 K to 473 K and flame-retardant effect of steam on benzene series. *Process Saf Environ Prot* 2020;137:328–39.
- Comandini A, Nativel D, Chaumeix N. Laminar Flame Speeds and Ignition Delay Times of Gasoline/Air and Gasoline/Alcohol/Air Mixtures: The Effects of Heavy Alcohol Compared to Light Alcohol. *Energy Fuels* 2021;35(18):14913–23.
- Fuller ME, Mousse-Rayaleh A, Chaumeix N, Goldsmith CF. Laminar flame speeds and ignition delay times for isopropyl nitrate and propane blends. *Combust Flame* 2022;242:112187.
- Grosseuvres R, Comandini A, Bentaib A, Chaumeix N. Combustion properties of H<sub>2</sub>/N<sub>2</sub>/O<sub>2</sub>/steam mixtures. *Proc Combust Inst* 2019;37(2):1537–46.
- Ranzi E, Frassoldati A, Grana R, Cuoci A, Faravelli T, Kelley AP, et al. Hierarchical and comparative kinetic modeling of laminar flame speeds of Hydrocarbon and Oxygenated fuels. *Prog Energy Combust Sci* 2012;38:468–501.
- Saggese C, Frassoldati A, Cuoci A, Faravelli T, Ranzi E. A wide range kinetic modeling study of pyrolysis and oxidation of benzene. *Combust Flame* 2013;160(7):1168–90.
- Nobili A, Cuoci A, Pejpichestakul W, Pelucchi M, Cavallotti C, Faravelli T. Modeling soot particles as stable radicals: a chemical kinetic study on formation and oxidation. Part I. Soot formation in ethylene laminar premixed and counterflow diffusion flames. *Combust Flame* 2022;243:12073.
- Stagni A, Frassoldati A, Cuoci A, Faravelli T, Ranzi E. Skeletal mechanism reduction through species-targeted sensitivity analysis. *Combust Flame* 2016;163:382–93.
- Cuoci A, Frassoldati A, Faravelli T, Ranzi E. OpenSMOKE++: An object-oriented framework for the numerical modeling of reactive systems with detailed kinetic mechanisms. *Comput Phys Commun* 2015;192:237–64.
- Mascarenhas VJ, Weber CN, Westmoreland PR. Estimating flammability limits through predicting non-adiabatic laminar flame properties. *Proc Combust Inst* 2021;38:4673–81.
- Bariki C, Halter F, Hesse R, Chauveau C, Pitsch H, Beeckmann J. Experimental measurements of laminar flame speeds for highly N<sub>2</sub>-diluted ethanol flames under microgravity conditions. *Proc Combust Inst* 2023;39(3):3929–38. <https://doi.org/10.1016/j.proci.2022.08.076>.
- Hesse R, Berger L, Bariki C, Hegetschweiler MJ, Linteris GT, Pitsch H, et al. Low global-warming-potential refrigerant CH<sub>2</sub>F<sub>2</sub> (R-32): Integration of a radiation heat loss correction method to accurately determine experimental flame speed metrics. *Proc Combust Inst* 2021;38(3):4665–72. <https://doi.org/10.1016/j.proci.2020.05.026>.
- Yu H, Han W, Santner J, Gou X, Sohn CH, Ju Y, et al. Radiation-induced uncertainty in laminar flame speed measured from propagating spherical flames. *Combust Flame Nov*. 2014;161(11):2815–24. <https://doi.org/10.1016/j.combustflame.2014.05.012>.
- Grosshandler WL. RADCAL: a narrow-band model for radiation calculations in a combustion environment. NIST Technical Note 1993;1402.
- Widmann JF. Evaluation of the Planck Mean Absorption coefficients for radiation transport through smoke. *Combust Sci Technol* 2003;175:2038–299.
- Wang G, Li Y, Yuan W, Zhou Z, Wang Y, Wang Z. Investigation on laminar burning velocities of benzene, toluene, and ethylbenzene up to 20 atm. *Combust Flame* 2017;184:312–23.
- Soloviova-Sokolova JV, Alekseev VA, Matveev SS, Chechet IV, Matveev SG, Konnov AA. Laminar burning velocities of benzene + air flames at room and elevated temperatures. *Fuel* 2016;175:302–9.
- Davis SG, Law CK. Determination of and fuel structure effects on laminar flame speeds of C<sub>1</sub> to C<sub>8</sub> hydrocarbons. *Combust Sci Technol* 1998;140:427–49.
- Fiumara A, Avella F. Sull'infiammabilità di Benzene, Toluene e Xileni. *Riv Dei Combust*, vol XXXV 1981;2–3:118–25.
- Rowley JR. Flammability limits, flash points, and their consanguinity: critical analysis, experimental exploration, and prediction. Ph.D. Thesis, Brigham Young University (Provo), 2010.
- Smooke DM, Miller JA, Kee RJ. Determination of adiabatic flame speeds by boundary value methods. *Combust Sci Technol Oct*. 1983;34(1–6):79–90. <https://doi.org/10.1080/00102208308923688>.
- Lewis B, von Elbe G. *Combustion, Flames and Explosions in Gases*. 2nd ed. New York: Academic Press; 1961.
- Stickling J. Experimentelle und theoretische Bestimmung des Inertgaseinflusses auf die Explosionsgrenzen organischer Verbindungen. Abschlussbericht Forschungsvorhaben AiF, vol. 10144, 1997, [Online]. Available: [www.chemsafe.ptb.de](http://www.chemsafe.ptb.de).
- Coward HF, Jones GW. Limits of flammability of gases and vapors. U.S. Bureau of Mines, Washington, USA, Bulletin 503; 1952.
- White AG. CXLVIII. - Limits for the propagation of flame in vapour-air mixtures. Part I. Mixtures of air and one vapour at the ordinary temperature and pressure. *J Chem Soc Trans* 1922;121:1244–70.
- Qi C, Yan X, Wang Y, Ning Y, Yu X, Hou Y, et al. Flammability limits of combustible gases at elevated temperatures and pressures: recent advances and future perspectives. *Energy Fuels* 2022;36:12896–916.
- Law CK, Egolfopoulos FN. A unified chain-thermal theory of fundamental flammability limits. *Symp Int Combust Jan*. 1992;24(1):137–44. [https://doi.org/10.1016/S0082-0784\(06\)80021-4](https://doi.org/10.1016/S0082-0784(06)80021-4).
- Santner J, Haas FM, Dryer FL, Ju Y. High temperature oxidation of formaldehyde and formyl radical: A study of 1,3,5-trioxane laminar burning velocities. *Proc Combust Inst* 2015;35(1):687–94. <https://doi.org/10.1016/j.proci.2014.05.014>.